J Mater Sci: Mater Electron (2021) 32:9106–9114

RF magnetron sputtering processed transparent conductive aluminum doped ZnO thin films with excellent optical and electrical properties

Chunhu Zhao[1], Junfeng Liu[2], Yixin Guo[1], Yanlin Pan[1], Xiaobo Hu[3], Guoen Weng[3], Jiahua Tao[1,*], Jinchun Jiang[1], Shaoqiang Chen[3], Pingxiong Yang[1,*], and Junhao Chu[1]

[1] *Ministry of Education Nanophotonics & Advanced Instrument Engineering Research Center, School of Physics and Electronic Science, East China Normal University, 500 Dongchuan Road, Shanghai 200241, China*
[2] *School of Electrical and Energy Engineering, Nantong Institute of Technology, 14 Yongxing Road, Nantong 226001, China*
[3] *School of Communication & Electronic Engineering, East China Normal University, 500 Dongchuan Road, Shanghai 200241, China*

Received: 22 December 2020
Accepted: 17 February 2021
Published online: 5 March 2021

ABSTRACT

Aluminum doped ZnO thin films (AZO), which simultaneously transmit light and conduct electrical current, are widely applied in photovoltaic devices. To achieve high performance AZO thin films, the effects of RF magnetron sputtering conditions on the optical and electrical properties of the films have been explored. The optimized AZO thin films exhibit strong (002) orientated growth with hexagonal wurtzite structure. The minimum resistivity of 0.9×10^{-3} Ω cm, the highest carrier concentration of 2.8×10^{20} cm^{-3}, the best Hall mobility of 22.8 cm^2 $(V\ s)^{-1}$ and average transmittance above 85% can be achieved at the optimum deposition condition of 0.2 Pa, 120 W and 200 °C. Considering the single parabolic band model, the bandgap shift by carrier concentration of the films can be attributed to the Burstein-Moss effect. The results indicate that RF magnetron sputtered AZO thin films are promising for solar cell applications relying on front contact layers.

1 Introduction

Aluminum doped ZnO (AZO) thin films, owing to low cost, wide bandgap and chemical stability, have been widely used as the front contact layers in state-of-the-art Cu(In,Ga)Se_2 (CIGS) and Cu_2ZnSnS_4 (CZTS) solar cells [1, 2]. For improving the device performance, AZO thin films demand high conductivity and optical transparency in visible and near infrared region. Through reducing the aluminum concentration, the optical properties of ZnO films can be largely enhanced. However, the lower aluminum concentration leads to lower carrier concentration,

Chunhu Zhao and Junfeng Liu have contributed equally to this work.

Address correspondence to E-mail: jhtao@phy.ecnu.edu.cn; pxyang@ee.ecnu.edu.cn

https://doi.org/10.1007/s10854-021-05578-2

which results in poorer conductivity [3]. In addition, the solar cell surface inside the contact openings might be damaged during the deposition of the AZO thin films [4]. Therefore, fabrication of high quality AZO thin films is critical to obtain high efficiency solar cells, and a soft, less damage fabrication method is essential to protect the thin N-layer of PN junction.

Over the past few years, many fabrication methods have been adopted to deposit the AZO thin films, including atomic layer deposition [5], chemical spray pyrolysis [6], sputtering [7] and sol-gel spin coating [8]. Among these, magnetron sputtering, which enables better control on high thickness uniformity over the large area [9], has become the most common technique to prepare AZO thin films for solar cell applications. To obtain high performance AZO thin films, substrate heating and annealing are efficient strategies. With increasing the deposition temperature, the crystallinity and the electrical resistivity of AZO thin films are improved [10, 11]. And high quality AZO thin films can be obtained by annealing under nitrogen atmosphere [12, 13]. However, the higher deposition and annealing temperature may result in the distortion of the underneath layers and facilitate the interlayer diffusion [14–16]. In order to fabricate solar cells, AZO thin films should be deposited at suitable temperature.

For light trapping purposes, the front AZO layer requires a rough surface texture and the transparent should be exceed 80% [17, 18]. The front contact thin films with rough surface texture can produce adequate light scattering effect, improving the light trapping capacity of photovoltaic devices. According to the reported literatures, the textured AZO layer can be obtained by diluted hydrochloric acid post-etching technique [19–21]. This method significantly enhanced the optical properties of AZO thin films, but the electrical properties deteriorated. This is because the acid reagents may damage the AZO layers, resulting in the decrease of the conductivity. Although the increased film thickness can improve the conductivity, the optical transparency is not ideal [22, 23]. Therefore, it is crucial to explore the RF magnetron sputtering technique without post-etching procedure for fabricating textured AZO thin films with excellent optical and electrical properties.

In this work, the AZO thin films with rough surface texture are fabricated by RF magnetron sputtering technique without annealing and post-etching process. By optimizing the deposition conditions, AZO thin films exhibit good crystallinity and preferable optical and electrical properties. We note that the working pressure, deposition power and substrate temperature play major roles in these performance issues. And we also confirm that the sputtering AZO thin films are highly texture with c-axis perpendicular to the substrate face with (002) preferential growth. We then discuss the effects of the deposition parameters on the resistivity and optical transmittance of AZO thin films. Our work highlights the RF magnetron sputtering technique in developing high performance AZO front contact layers for solar cell applications.

2 Experimental

2.1 Fabrication of AZO thin films

AZO thin films were fabricated on soda-lime glass substrates by RF magnetron sputtering. The glass substrates were respectively cleaned by acetone, ethanol and distilled water. Then, they were dried by nitrogen gas before putting into the vacuum chamber. The vacuum chamber was pumped down to below 5×10^{-4} Pa via a turbo molecular pump. The mass ratio of Al_2O_3 and ZnO was 2:98, and the diameter of ceramic planar target was 50 mm. The distance between target and substrate was set as 65 mm, and the deposition time was kept as 45 min. Argon gas with high purity of 99.999% was used as sputtering gas with the pressure of 0.2–1.0 Pa. The flux of argon gas was controlled with mass flow controller and set as 30 sccm.

2.2 Characterization of AZO thin films

The thickness of AZO thin films was measured by Dektak XT Stylus Surface Profiling System (Veeco, Dektak 6M). The crystalline structures of thin films were characterized by X-ray diffraction using Cu Kα radiation (D/MAX-2550, Rigaku Co.). The surface morphologies were recorded by a field emission scanning electron microscopy (FESEM: Philips XL30FEG). The electrical resistivity, Hall mobility and carrier concentration were deduced from Hall measurements using a Van der Pauw configuration. And the optical transmission spectra of the thin films were recorded by UV-Visible-NIR Cary 5000 Varian double beam spectrophotometers. For transmittance

measurements, the beam was passed through the glass substrate into thin film, and a blank glass slide was kept in the path of the reference beam for compensation. Note that all the measurements were performed at room temperature.

3 Results and discussion

3.1 Morphology and crystal structure of AZO thin films

X-ray diffraction (XRD) analyses were performed on all the AZO thin films using glass substrates at various deposition conditions, as shown in Fig. 1a–c. Here, we set a baseline recipe as: working pressure was 0.2 Pa, RF power was 100 W, and substrate temperature was ambient temperature. It can be seen from Fig. 1a–c that the diffraction peaks of AZO thin films match well with the standard XRD pattern of ZnO (PDF#36-1451), demonstrating that the hexagonal wurtzite crystal structures were formed. It is well know that the sputtering ZnO thin films are highly texture with a preferential growth perpendicular to the substrate [24–26]. Our experiments represent the similar results, especially for the films fabricated in low working pressure (< 0.6 Pa), moderate RF sputtering power (50–100 W) and suitable substrate temperature (100–200 °C), which have a strong diffraction peak of (002) at 2θ value of 34.4°.

Figure 1a reveals that the crystallization of AZO thin films becomes worse when the working pressure increases from 0.2 to 1.0 Pa. The diffraction peaks at 2θ value of 36.2° suggest that some grains are crystalline with orientation along (101) plane. It can be ascribed that the higher working pressure may raise the deposition rate and cause the alteration of the mean free path of the sputtered particles [21], resulting in poor crystallization. XRD patterns of AZO thin films deposited at various RF sputtering power are shown in Fig. 1b. The intensity and full width at half maximum of the diffraction peaks indicate that the crystallite size changes with the sputtering power, and the similar experimental phenomenon was also observed in the literature [13].

We can also find that, for AZO thin films deposited at the substrate temperature ranging from ambient temperature to 200 °C, the intensity and sharpness of the (002) peak increased, and the other peaks disappeared (see Fig. 1c). That's to say, higher substrate temperature is conducive to improve the crystallization of the thin films. According to the literature, with the increase of the deposition temperature, the mobility of the growing species on substrate is greatly enhanced [7, 27, 28]. Therefore, the nucleation of the growing species is improved, further promoting the crystallinity and reducing the defects of AZO thin films. As verified with grain size, calculated by the Scherrer formula based on the (002) peak [6, 8], it increases from 32.0 to 34.1 nm with the substrate temperature varying from 100 to 200 °C.

The surface morphology of AZO thin films plays a critical role in the photovoltaic device performance. The SEM micrograph of the film, which is deposited at 0.2 Pa, 120 W and 200 °C, is presented in Fig. 1d. It can be clearly observed that the film has a compact and homogeneous self-textured surface. For the purpose of absorbing wider wavelength region, the rough transparent conducting oxide (TCO) thin films are used to enhance light scattering effects. Compared to the reference TCO thin films, there has a reduction in parasitic absorption for the textured films because it has better transparency and maintains excellent light trapping qualities [29, 30]. In our experiments, the electrical and optical properties of AZO thin films are also analyzed in the following.

3.2 Electrical properties of AZO thin films

Electrical properties of AZO thin films deposited at different conditions are shown in Fig. 2 and Table 1. We firstly carried out the measurements of the deposition rate of the films under various deposition conditions. From Fig. 2a, it can be found that the substrate temperature and working pressure have a slight effect on the deposition rate, where we set the ambient temperature as 50 °C. Unlike the above two parameters, RF sputtering power can strongly affect the deposition rate of AZO thin films. As described in the literature, the faster deposition rate can be achieved by increasing RF sputtering power, further improving crystalline size [9]. This phenomenon is in good agreement with the XRD results (see Fig. 1b).

The effects of the deposition conditions on carrier concentration (N), Hall mobility (μ) and resistivity (ρ) of AZO thin films are demonstrated in Fig. 2b–d. From Fig. 2b, we find that there has a V-shape curve of electrical properties for AZO thin films deposited at the working pressure ranging from 0.2 to 1.0 Pa. When the working pressure increases to 0.6 Pa, the

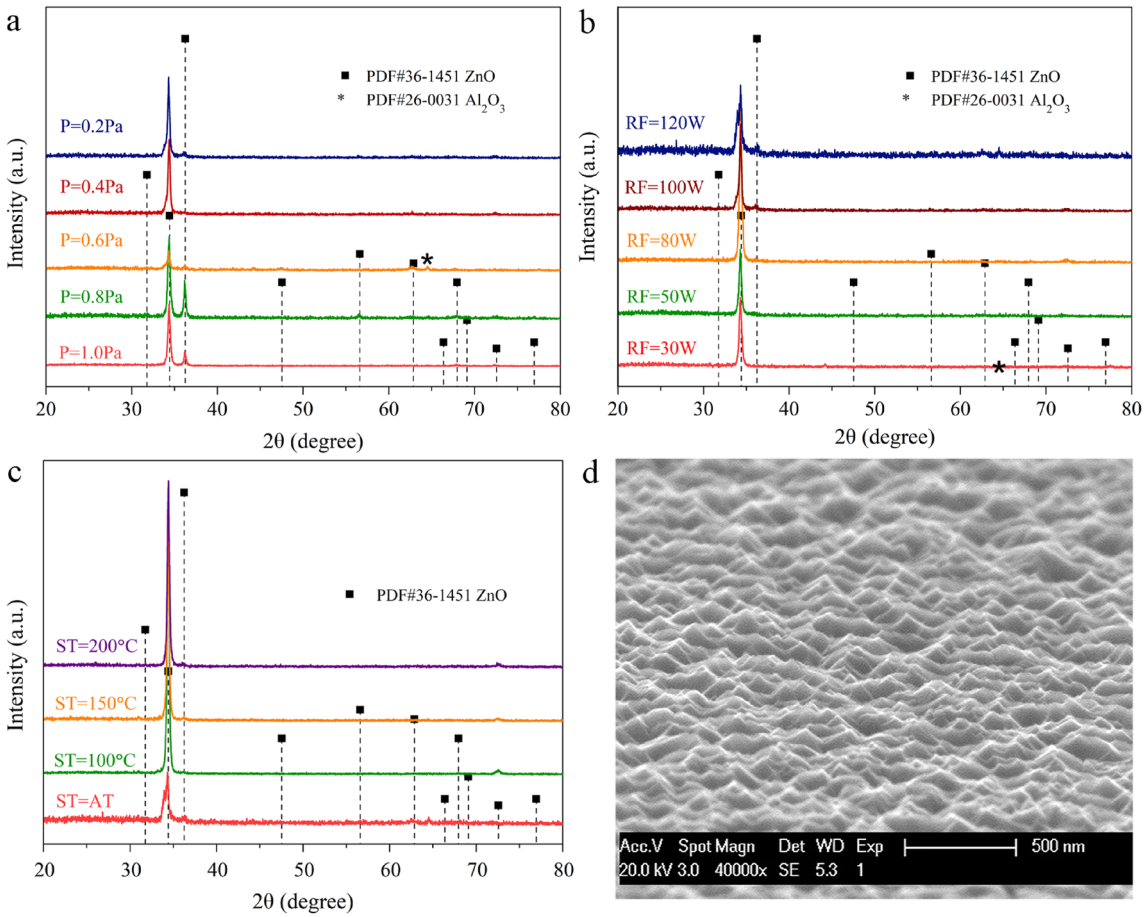

Fig. 1 Morphology and crystal structure of AZO thin films. **a** XRD patterns of the films deposited at various working pressure. **b** XRD patterns of the films with variation of RF sputtering power. **c.** Variation of XRD patterns of the films with the substrate temperature (ST). **d** Surface morphology of the film deposited at optimum deposition conditions

deposited thin films have the highest resistivity of ~1.9 × 10^{-2} Ω cm, the lowest carrier concentration (0.8 × 10^{20} cm^{-3}) and Hall mobility (4.2 cm^2 $(V\ s)^{-1}$). The electrical properties are closely associated with the film crystallinity, which is evident from the XRD results of AZO thin films under the working pressure (see Fig. 1a). At lower working pressure, the film crystallinity is much better than that deposited under higher working pressure, which indicates better electrical properties.

Unlike the deposition parameter of working pressure, the resistivity decreases as the increasing of RF sputtering power and substrate temperature, but the Hall mobility and carrier concentration increase. As shown in Fig. 2c, when PF sputtering power increases from 30 W to 80 W, the resistivity decreases quickly, which may be mainly caused by increment of film thickness [23]. Then, there has a slight decrease as PF sputtering power keeps rising. From Fig. 2d, the resistivity of AZO thin films decreases gradually from 3 × 10^{-3} to 0.9 × 10^{-3} Ω cm with the substrate temperature varying from 50 to 200 °C, while the films have higher carrier concentrations and Hall mobilities at higher substrate temperature. According to the reported literature, the reduction in resistivity at higher deposition temperature is related to the improved film crystallinity and the growth of grain size, which will result in reducing the scattering of carrier transport [31–33]. Overall, the minimum resistivity of 0.9 × 10^{-3} Ω cm, the highest carrier concentration of 2.8 × 10^{20} cm^{-3} and the best Hall mobility of 22.8 cm^2 $(V\ s)^{-1}$ can be obtained for AZO thin films deposited at the optimum deposition condition of 0.2 Pa, 120 W and 200 °C.

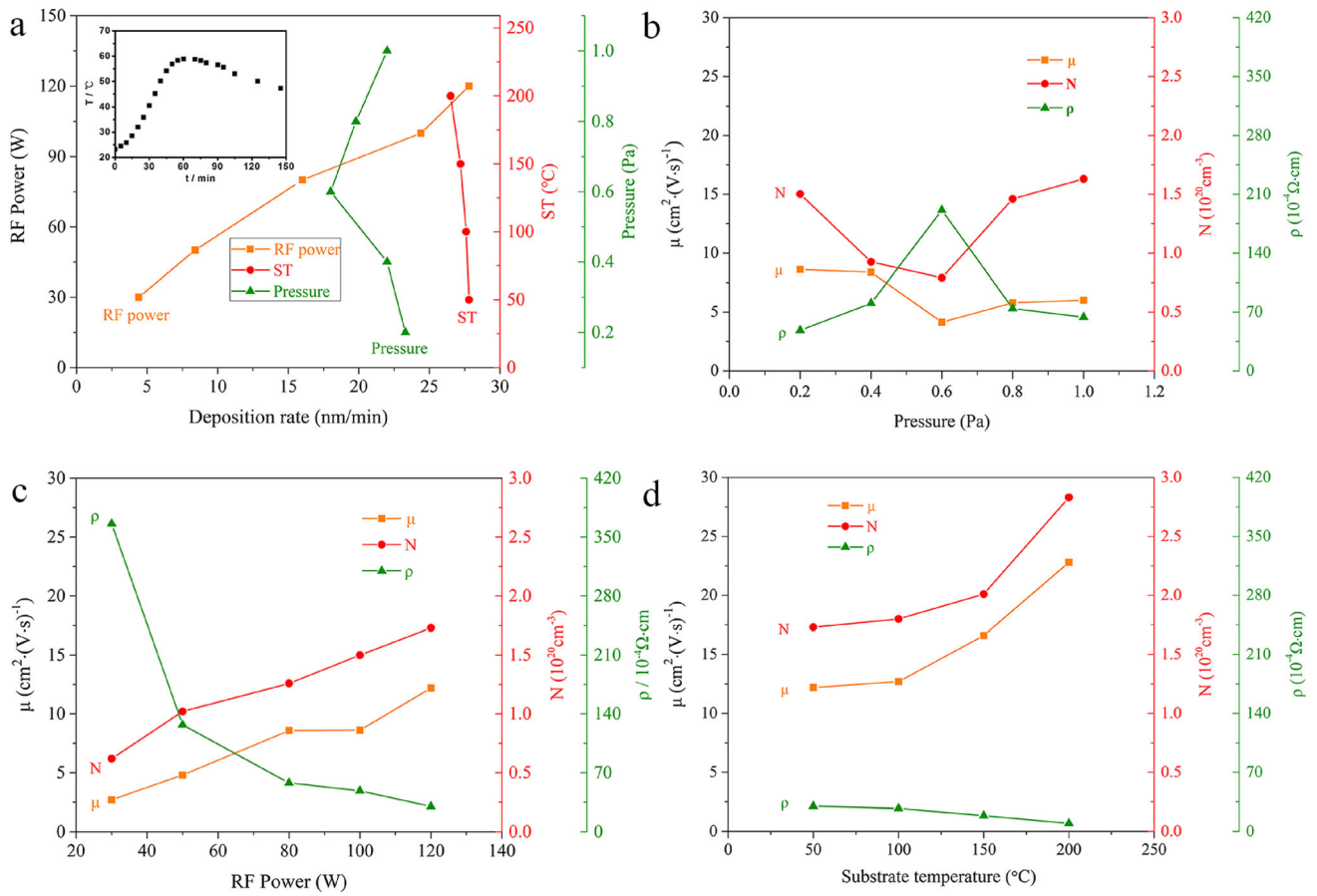

Fig. 2 Electrical properties of AZO thin films. **a** The deposition rate of AZO thin films varying with working pressure, substrate temperature and RF sputtering power. Inset: the substrate temperature monitor t-T curve. **b** Carrier concentration (N), Hall mobility (μ) and resistivity (ρ) of the films deposited under different working pressure. **c** Carrier concentration, resistivity and Hall mobility as a function of RF sputtering power for the films. **d** The dependence of the resistivity, Hall mobility and carrier concentration of the films on substrate temperature

3.3 Optical properties of AZO thin films

To achieve the optical properties of AZO thin films, we carried out the transmittance measurements. The optical properties of thin films varying with deposition parameters are summarized in Table 2 and Fig. 3, which are discussed in detail in the following sections. Fig. 3a shows the transmittance spectra of the films deposited at various RF sputtering power. In the wavelength range of 400–1100 nm, the films are highly transparent, and the average transmittance is up to 85%. It can also be found that the spectrums of as-deposited films exhibit different interference fringes pattern, which is related to the film thickness [34]. The film thickness has a strong influence on the optical bandgap. The absorption coefficient (α) can be calculated using the optical transmittance (T) of AZO thin films, which is described by the relation of $T=exp(-\alpha d)$ [7], where d is the film thickness. Then, the optical bandgaps (E_g) of AZO thin films are determined using the relation of $(\alpha h\upsilon)^2=h\upsilon-E_g$ by extrapolating $(\alpha h\upsilon)^2$ plot linearly with the incident photon energy ($h\upsilon$) for direct transition [9].

Based on the above calculation method, the optical bandgaps of AZO thin films deposited at different RF sputtering power can be obtained, as shown in Fig. 3b. The bandgap of the films increases from 3.28 to 3.39 eV with the increase of RF sputtering power. The widening bandgap may be caused by the increased carrier concentration (see Fig. 3c) in accordance to Burstein-Moss effect [35]. From Fig. 3d, it can be seen that the transmittance of the films deposited at different substrate temperature is also around 85% in the visible region. Compared with the films deposited at various RF sputtering power, the spectrums of as-deposited films exhibit the same

Table 1 Electrical properties of AZO thin films varying with deposition parameters

Deposition parameters			Electrical properties		
Power (W)	Pressure (Pa)	Substrate temperature (°C)	Resistivity ($\times 10^{-4}$ Ω cm)	Hall mobility (cm^2 $(V s)^{-1}$)	Carrier concentration ($\times 10^{20}$ cm^{-3})
100	0.2	RT	48.26	8.69	1.51
100	0.4	RT	80.51	8.41	0.93
100	0.6	RT	190.99	4.19	0.79
100	0.8	RT	74.20	5.82	1.47
100	1.0	RT	63.90	5.99	1.64
30	0.2	RT	366.49	2.81	0.62
50	0.2	RT	127.64	4.84	1.02
80	0.2	RT	57.44	8.55	1.27
100	0.2	RT	48.26	8.69	1.51
120	0.2	RT	31.50	12.15	1.73
100	0.2	RT	48.26	8.69	1.51
100	0.2	50	30.95	12.23	1.73
100	0.2	100	28.64	12.68	1.80
100	0.2	150	18.33	16.50	2.01
100	0.2	200	9.64	22.76	2.84

Table 2 Optical properties of AZO thin films varying with deposition parameters

Deposition parameters			Optical properties	
Power (W)	Pressure (Pa)	Substrate temperature (°C)	Transmittance (400–1100 nm, %)	Bandgap (eV)
30	0.2	RT	92.54	3.28
50	0.2	RT	90.71	3.32
80	0.2	RT	89.08	3.36
100	0.2	RT	88.90	3.38
120	0.2	RT	83.92	3.39
120	0.2	100	85.32	3.41
120	0.2	150	88.10	3.43
120	0.2	200	85.76	3.52

interference fringes pattern. But for NIR spectra, there has an obvious drop in the transmittance, and this may be ascribed to the strengthening of light scattering and absorption [36]. The bandgaps of the films, shown in Fig. 3e, are 3.39 eV, 3.41 eV, 3.43 eV and 3.52 eV with substrate temperature of AT, 100 °C, 150 °C and 200 °C, respectively. We assumed that not only the increase of carrier concentration (see Fig. 3f), but also internal stress and phase purity [16, 37], can affect the optical bandgap of AZO thin films.

Dependence of carrier concentration and optical bandgap of AZO thin films on RF sputtering power and substrate temperature indicates that absorption edges of the films are strongly dependent on carrier concentration. According to Burstein-Moss effect, in the doped *n*-type semiconductor, the optical bandgap E_g has contribution from free charge carriers E_0 and the donor atoms ΔE_{MB}. Therefore, considering the single parabolic band model, the energy shift by carrier concentration of AZO thin films can be expressed as [38–40]:

$$\Delta E_{MB} = \frac{h^2}{8m^*}\left(\frac{3N}{\pi}\right)^{2/3}$$

where, m^* is the electron effective mass in the conduction band, h is the Planck constant (6.626×10^{-34} m^2 kg s^{-1}), and N is the carrier concentration. To further investigate the relationship of N and ΔE_{MB},

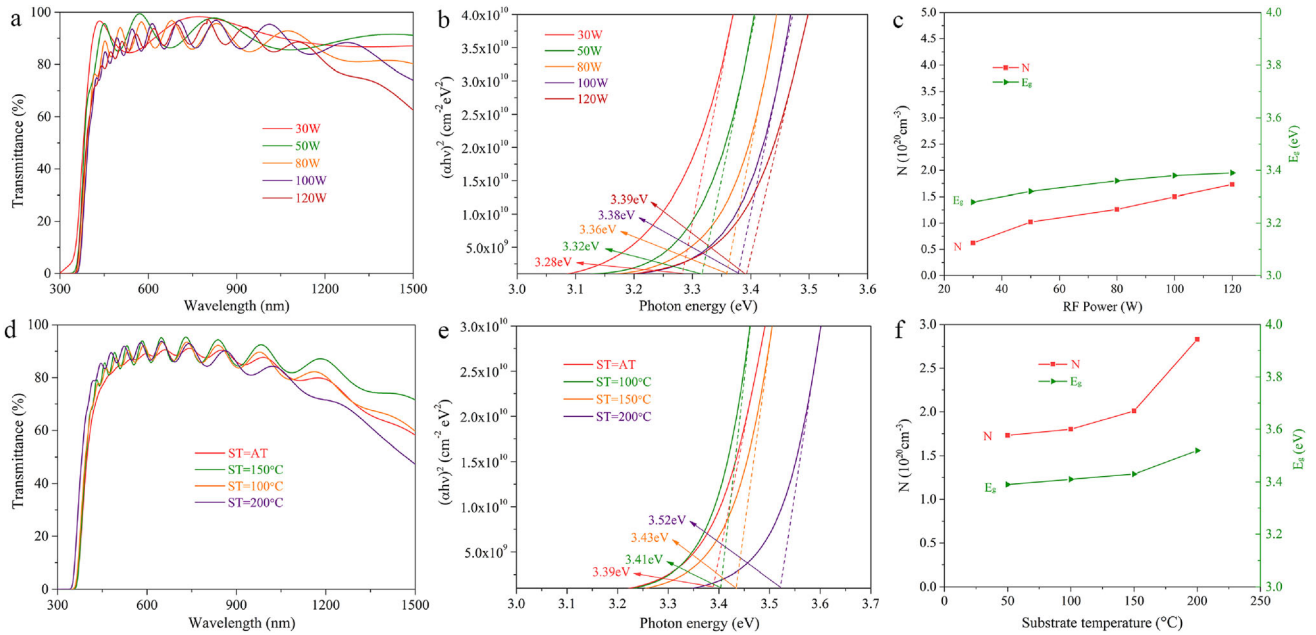

Fig. 3 Optical properties of AZO thin films. **a–c** Transmission, bandgaps and N-E_g curves of the films deposited at various RF sputtering power. **b–d** The effects of substrate temperature on transmission, bandgaps and N-E_g curves of the films

the N-ΔE_{MB} curve is plotted in Fig. 4. Note that the solid curve in Fig. 4 is calculated using the above equation. It can be seen that the ΔE_{MB} exhibits a good linear relation with the carrier concentration, which indicates that the Burstein-Moss theory of band filling can fully interpret the bandgap shift of AZO thin films. Similar results are also reported by Zhu et al. and they demonstrate that the increase of optical bandgap for AZO thin films can be mainly attributed to the Burstein-Moss effect, although other effects also appear [15].

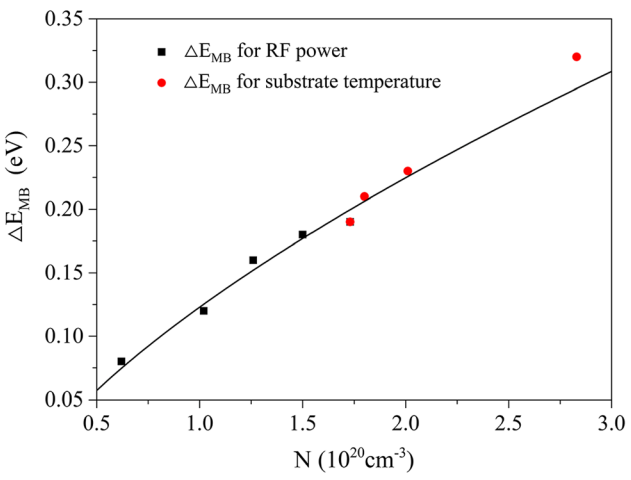

Fig. 4 Bandgap energy shift as a function of carrier concentration in AZO thin films. The solid curve shows the fitting result using the Burstein-Moss theory. The black squares and red circles show the experimental data

4 Conclusion

In summary, AZO thin films are successfully deposited on glass substrate using RF magnetron sputtering method. The effects of working pressure, RF sputtering power and substrate temperature on optical and electrical properties have been investigated systemically. Through structural characterization, it can be found that the films are polycrystalline structure with a hexagonal wurtzite structure. The (002) orientated growth films can be easily fabricated with substrate temperature higher than 100 °C. The deposition rate of the films is strongly depended on RF sputtering power and working pressure. Substrate temperature slightly affects the deposition rate, but plays an important role in the film crystallinity. In addition, more powerful sputtering energy and elevated substrate temperature are conducive to obtain better mobility and higher carrier concentration, further leading to lower resistivity. Considering the single parabolic band model, the bandgap shift by carrier concentration of the films can be attributed to the Burstein-Moss effect. In general, the minimum resistivity of 0.9×10^{-3} Ω cm, the highest carrier concentration of 2.8×10^{20} cm^{-3}, the

best Hall mobility of 22.8 cm^2 $(V\ s)^{-1}$ and the average transmittance of 85% can be achieved at the optimum deposition condition of 0.2 Pa, 120 W and 200 °C. The above results indicate that RF magnetron sputtered AZO thin films with rough surface texture can be considered as potential front contact layers for solar cell applications.

Acknowledgements

This work was financially supported by the National Natural Science Foundation of China (Grant Nos. 61474045 and 61704057), Natural Science Foundation of Shanghai (Grant Nos. 20ZR1417400) and General Projects of Natural Science Research in Universities of Jiangsu Province (Grant Nos. 17KJB480001).

Declarations

Conflict of interest We declare that we have no financial and personal relationships with other people or organizations that can inappropriately influence our work, there is no professional or other personal interest of any nature or kind in any product, service and/or company that could be construed as influencing the position presented in, or the review of, the manuscript entitled.

References

1. P. Jackson, R. Wuerz, D. Hariskos, E. Lotter, W. Witte, M. Powalla, Effects of heavy alkali elements in Cu(In, Ga)Se2 solar cells with efficiencies up to 22.6%. Phys. Status Solidi RRL **10**, 583–586 (2016)
2. K.J. Yang, S. Kim, S.Y. Kim, K. Ahn, D.H. Son, S.H. Kim, S.J. Lee, Y. Kim, S.N. Park, S.J. Sung, D.H. Kim, T. Enkhbat, J. Kim, C.W. Jeon, J.K. Kang, Flexible $Cu_2ZnSn(S, Se_)4$ solar cells with over 10% efficiency and methods of enlarging the cell area. Nat. Commun. **10**, 2959 (2019)
3. Y.H. Kim, J. Jeong, K.S. Lee, J.K. Park, Y.J. Baik, T.Y. Seong, W.M. Kim, Characteristics of ZnO: Al thin films co-doped with hydrogen and fluorine. Appl. Surf. Sci. **256**, 5102–5107 (2010)
4. F. Werner, B. Veith-Wolf, M. Melchiorre, F. Babbe, J. Schmidt, S. Siebentritt, Ultra-thin passivation layers in Cu(In, Ga)S_e2 thin-film solar cells: full-area passivated front contacts and their impact on bulk doping. Sci. Rep. **10**, 7530 (2020)
5. M.L. Lin, J.M. Huang, C.S. Ku, C.M. Lin, H.Y. Lee, J.Y. Juang, High mobility transparent conductive Al-doped ZnO thin films by atomic layer deposition. J. Alloys Compd. **727**, 565–571 (2017)
6. M. Kumar, B. Singh, P. Yadav, V. Bhatt, M. Kumar, K. Singh, A.C. Abhyankar, A. Kumar, J.H. Yun, Effects of structural defects, surface roughness on sensing properties of Al doped ZnO thin films deposited by chemical spray pyrolysis technique. Ceram. Int. **43**, 3562–3568 (2017)
7. P. Tang, B. Li, L. Feng, The optical and electrical properties of ZnO: Al thin films deposited at low temperatures by RF magnetron sputtering. Ceram. Int. **44**, 4154–4157 (2018)
8. H. Aydin, F. Yakuphanoglu, C. Aydin, Al-doped ZnO as a multifunctional nanomaterial: structural, morphological, optical and low-temperature gas sensing properties. J. Alloys Compd. **773**, 802–811 (2019)
9. S.R. Dhage, A.C. Badgujar, Transparent conducting Al:ZnO thin films on large area by efficient cylindrical rotating DC magnetron sputtering. J. Alloys Compd. **763**, 504–511 (2018)
10. J. Nomoto, T. Hirano, T. Miyata, T. Minami, Preparation of Al-doped ZnO transparent electrodes suitable for thin-film solar cell applications by various types of magnetron sputtering depositions. Thin Solid Films **520**, 1400–1406 (2011)
11. D.K. Kim, H.B. Kim, Investigation of ZnO: Al thin films sputtered at different deposition temperatures. J. Korean Phys. Soc. **66**, 1581–1585 (2015)
12. W. Yang, Z. Wu, Z. Liu, A. Pang, Y.L. Tu, Z.C. Feng, Room temperature deposition of Al-doped ZnO films on quartz substrates by radio-frequency magnetron sputtering and effects of thermal annealing. Thin Solid Films **519**, 31–36 (2010)
13. D. Podobinski, S. Zanin, A. Pruna, D. Pullini, Effect of annealing and room temperature sputtering power on optoelectronic properties of pure and Al-doped ZnO thin films. Ceram. Int. **39**, 1021–1027 (2013)
14. Z.A. Wang, J.B. Chu, H.B. Zhu, Z. Sun, Y.W. Chen, S.M. Huang, Growth of ZnO: Al films by RF sputtering at room temperature for solar cell applications. Solid-State Electron. **53**, 1149–1153 (2009)
15. B.L. Zhu, J. Wang, S.J. Zhu, J. Wu, D.W. Zeng, C.S. Xie, Thickness study of AZO films by RF sputtering in $Ar+H_2$ atmosphere at room temperature. Phys. Status Solidi A **209**, 1251–1258 (2012)
16. M. Asemi, M. Ahmadi, M. Ghanaatshoar, Preparation of highly conducting Al-doped ZnO target by vacuum heat-treatment for thin film solar cell applications. Ceram. Int. **44**, 12862–12868 (2018)
17. Z. Ghorannevis, E. Akbarnejad, A. Salar Elahi, M. Ghoranneviss, Magnetron sputtered AZO thin film preparation for the solar cell applications. J. Inorg. Organomet Polym. **25**, 1486–1489 (2015)

18. X. Yan, W. Li, A.G. Aberle, S. Venkataraj, Textured AZO for thin-film Si solar cells: towards understanding the effect of AZO film thickness on the surface texturing properties. Procedia Eng. **139**, 134–139 (2016)
19. W.L. Lu, K.C. Huang, C.H. Yeh, C.I. Hung, M.P. Houng, Investigation of textured Al-doped ZnO thin films using chemical wet-etching methods. Mater. Chem. Phys. **127**, 358–363 (2011)
20. Y. Wang, X. Zhang, L. Bai, Q. Huang, C. Wei, Y. Zhao, Effective light trapping in thin film silicon solar cells from textured Al doped ZnO substrates with broad surface feature distributions. Appl. Phys. Lett. **100**, 263508 (2012)
21. Y. Wang, J. Song, L. Bai, F. Yang, B. Han, Y. Guo, B. Dai, Y. Zhao, X. Zhang, Management of light trapping capability of AZO film for Si thin film solar cells-via tailoring surface texture. Sol. Energy Mater. Sol. Cells **179**, 401–408 (2018)
22. A. Rayerfrancis, P.B. Bhargav, N. Ahmed, S. Bhattacharya, B. Chandra, S. Dhara, Sputtered AZO thin films for TCO and back reflector applications in improving the efficiency of thin film a-Si: H solar cells. Silicon **9**, 31–38 (2017)
23. C. Ma, X. Lu, B. Xu, F. Zhao, X. An, B. Li, L. Sun, J. Jiang, Y. Chen, J. Chu, Effects of sputtering parameters on photoelectric properties of AZO film for CZTS solar cell. J. Alloys Compd. **774**, 201–209 (2019)
24. E.M. Mkawi, K. Ibrahim, M.K.M. Ali, M.A. Farrukh, A.S. Mohamed, The effect of dopant concentration on properties of transparent conducting Al-doped ZnO thin films for efficient Cu_2ZnSnS_4 thin-film solar cells prepared by electrodeposition method. Appl. Nanosci. **5**, 993–1001 (2015)
25. Z. Du, X. Liu, Y. Zhang, J. Shuai, H. Li, Robust AZO/i-ZnO bilayer front contact for high-performance thin film solar cells. RSC Adv. **6**, 108067–108074 (2016)
26. P. Saravanan, A. Gnanavelbabu, P. Pandiaraj, Effect of pre-annealing on thermal and optical properties of ZnO and Al-ZnO thin films. Int. J. Nanosci. **17**, 1760017 (2018)
27. B. Li, J. Liu, G. Xu, R. Lu, L. Feng, J. Wu, Development of pulsed laser deposition for CdS/CdTe thin film solar cells. Appl. Phys. Lett. **101**, 153903 (2012)
28. Y. Lu, S. Wang, M. Yang, X. Xu, Q. Li, Comparative study of AZO and ITO thin film sputtered at different temperatures and their application in Cu_2ZnSnS_4 solar cells. J. Mater. Sci. Mater. Electron. **29**, 17525–17532 (2018)
29. M. Boccard, C. Battaglia, S. Hanni, K. Soderstrom, J. Escarre, S. Nicolay, F. Meillaud, M. Despeisse, C. Ballif, Multiscale transparent electrode architecture for efficient light management and carrier collection in solar cells. Nano Lett. **12**, 1344–1348 (2012)
30. X. Liang, B. Liu, L. Bai, J. Liang, H. Gao, Y. Zhao, X. Zhang, Periodically textured metal electrodes: large-area fabrication, characterization, simulation, and application as efficient back-reflective scattering contact-electrodes for thin-film solar cells. J. Mater. Chem. A **2**, 13259–13269 (2014)
31. Z. Baji, Z. Labadi, Z.E. Horvath, I. Barsony, Structure and morphology of aluminium doped Zinc-oxide layers prepared by atomic layer deposition. Thin Solid Films **520**, 4703–4706 (2012)
32. H.Y. Liu, V. Avrutin, N. Izyumskaya, U. Ozgur, A.B. Yankovich, A.V. Kvit, P.M. Voyles, H. Morkoc, Electron scattering mechanisms in GZO films grown on a-sapphire substrates by plasma-enhanced molecular beam epitaxy. J. Appl. Phys. **111**, 103713 (2012)
33. P. Genevee, F. Donsanti, G. Renou, D. Lincot, Study of the aluminum doping of zinc oxide films prepared by atomic layer deposition at low temperature. Appl. Surf. Sci. **264**, 464–469 (2013)
34. Z. Kan, Z. Wang, Y. Firdaus, M. Babics, H.N. Alshareef, P.M. Beaujuge, Atomic-layer-deposited AZO outperforms ITO in high-efficiency polymer solar cells. J. Mater. Chem. A **6**, 10176–10183 (2018)
35. Y. Kim, W. Lee, D.R. Jung, J. Kim, S. Nam, H. Kim, B. Park, Optical and electronic properties of post-annealed ZnO: Al thin films. Appl. Phys. Lett. **96**, 171902 (2010)
36. X.Y. Li, H.J. Li, Z.J. Wang, H. Xia, Z.Y. Xiong, J.X. Wang, B.C. Yang, Effect of substrate temperature on the structural and optical properties of ZnO and Al-doped ZnO thin films prepared by dc magnetron sputtering. Opt. Commun. **282**, 247–252 (2009)
37. B.L. Zhu, M. Xie, J. Wang, X.W. Shi, J. Wu, D.W. Zeng, C.S. Xie, Comparative study on effects of H_2 flux on structure and properties of Al-doped ZnO films by RF sputtering in $Ar+H_2$ ambient at two substrate temperatures. Ceram. Int. **40**, 12093–12104 (2014)
38. A.V. Singh, R.M. Mehra, A. Yoshida, A. Wakahara, Doping mechanism in aluminum doped zinc oxide films. J. Appl. Phys. **95**, 3640–3643 (2004)
39. J.G. Lu, S. Fujita, T. Kawaharamura, H. Nishinaka, Y. Kamada, T. Ohshima, Z.Z. Ye, Y.J. Zeng, Y.Z. Zhang, L.P. Zhu, H.P. He, B.H. Zhao, Carrier concentration dependence of band gap shift in *n*-type ZnO: Al films. J. Appl. Phys. **101**, 083705 (2007)
40. A. Paulson, N.A. Muhammed Sabeer, P.P. Pradyumnan, Enhancement of optical and thermoelectric properties in dysprosium doped ZnO thin films as an impact of non-parabolic band structure. Mater. Sci. Eng. B **262**, 114745 (2020)